A SINDO1 Study of Photoisomerization and Photofragmentation of Cyclopentanone

Peter L. Müller-Remmers, P. C. Mishra,† and Karl Jug*

Contribution from Theoretische Chemie, Universität Hannover, 3000 Hannover 1, Federal Republic of Germany. *Received July 13, 1983*

Abstract: The photoisomerization of cyclopentanone to 4-pentenal and the photofragmentation to cyclobutane and carbon monoxide or to two ethylene and carbon monoxide was investigated by the SINDO1 method including configuration interaction (CI). Structures and energies of all pertinent ground and excited states as well as transition states and intermediates were calculated. The mechanism for all reactions involves excitation to S_1 and intersystem crossing to T_1 or T_2. The triplets lead to diradical intermediates from which further reaction to the products takes place. The dependence of product distribution on excitation wavelength is discussed.

1. Introduction

The results of experimental studies on the photochemistry of cyclopentanone (CP) and other cyclic ketones have been reported in several papers.[1-15] But from the point of view of the mechanisms involved, the opinions of different authors are quite divergent.[2,4,6,8] For example, even as broad an issue as to whether or not the first triplet excited state of CP is important in its photochemistry is disputed according to the available literature[2,4,8] and has only recently been accepted.[15]

Recent studies have established[8,10,15] that, in the gaseous phase, CP undergoes photodecomposition primarily into cyclobutane (CB), ethylene (Et), and CO at lower excitation wavelengths ($\lambda_{ex} \simeq 257$ nm), whereas at wavelengths of $\lambda_{ex} \simeq 320$ nm, it mainly undergoes photoisomerization to 4-pentenal (4P). In the liquid phase the photolysis of CP yields 4P only. According to the most recent experimental views on this matter, the photochemistry of CP is dominated by the intersystem crossing $S_1 \rightsquigarrow T_1$ and vibrational energy content of the molecule.[15]

It has been observed that 20-30% of the excited CP molecules also revert to the ground state without any change;[5] the mechanism of this phenomenon is not at all understood.[5,15,17] A knowledge of the features of potential energy hypersurfaces (PES) is in general of great value in understanding the roles of various possible processes.[16,17] In the present work, we have investigated the hypersurface features relevant to the photoisomerization of CP to 4P and to the photofragmentation of CP to CB, Et plus CO, following excitations of the former molecule to its first excited singlet states. No earlier work of this type is available on this problem. However, a calculation of the singlet transitions of some saturated ketones using the CNDO/S-CI and other similar methods have been reported.[12]

2. Method of Calculations

The SINDO1 semiempirical method (details are available elsewhere[18]) was used for the calculations in conjunction with configuration interaction (CI). Starting from CP in the ground state, we considered all single vertical excitations from the three highest occupied orbitals to the three lowest unoccupied orbitals and the double excitation from HOMO to LUMO in the CI expansion. The Newton-Raphson method[18,19] was used to obtain extrema on the excited PESs. All internal coordinates were optimized for minima and saddle points on the two lowest singlet and triplet surfaces. The procedure of calculation was described in detail in a recent paper on excited states.[20] For reaction pathways we considered the variation of energy of a selected excited state along a guiding coordinate which describes a significant geometrical change from reactant to intermediate or product. For fixed values of this coordinate, all other internal coordinates were subjected to energy minimization. Together with this selected state the vertical energy values of one higher and all lower excited states of the same spin were calculated. The corresponding state of the complementary spin, i.e., singlet for triplet and vice versa, was also considered.

Table I. Energies (eV) of Relevant States on Potential Surfaces for Cyclopentanone Reaction

vertical		primary adiabatic		secondary adiabatic		vertical	
R_0	0			TS_0	3.58	P_0	1.02
$^3R_1(n-\pi^*)$	4.39	$^3I_1$	2.20	$^{1,3}D$	3.21	$^3P_1(n-\pi^*_{CO})$	5.37
		$^3I_1'$	2.65	$^{1,3}D'$	3.77		
		$^3I_1''$	3.35				
$R_1(n-\pi^*)$	4.77	$R_1(n-\pi^*)$	4.51	I_1	6.40	$P_1(n-\pi^*_{CO})$	5.68
$^3R_2(n-\sigma^*)$	4.99					$^3P_2(n-\pi^*_{CC})$	5.61
$R_2(n-\sigma^*)$	7.40					$P_2(n-\sigma^*)$	8.08

3. Results and Discussion

3.1. Spectral Transitions. Calculated excitation energies are presented in Table I. Here we have introduced the following notation. Singlet states on the ground state surface S_0 are called R_0 for reactant CP, P_0 for product 4P, and TS_0 for transition state. Singlet states on the excited surfaces S_1 and S_2 are called R_1 and R_2 for reactants; I_1 is for intermediate. The triplet surfaces have states $^3R_1$, $^3R_2$ and intermediates $^3I_1$, $^3I_1'$, $^3I_1''$. There are two diradical situations $^{1,3}D$ and $^{1,3}D'$ for fragmentation where ground state surface S_0 and first excited triplet surface T_1 are degenerate. In the equilibrium geometries of the states R_0 and R_1 the highest occupied molecular orbital (HOMO) is localized on oxygen, and

† Alexander von Humboldt Fellow, 1981-82. Permanent address: Department of Physics, Banaras Hindu University, Varanasi-221005, India.

(1) Blacet, F. E.; Miller, A. *J. Am. Chem. Soc.* **1957**, *79*, 4327.
(2) Srinivasan, R. *J. Am. Chem. Soc.* **1959**, *81*, 1546; **1961**, *83*, 4344, 4348.
(3) La Paglia, S. R.; Roquitte, B. C. *J. Phys. Chem.* **1962**, *66*, 1739.
(4) La Paglia, S. R.; Roquitte, B. C. *Can. J. Chem.* **1963**, *41*, 287.
(5) Srinivasan, R. *Adv. Photochem.* **1963**, *1*, 83.
(6) Udverhazi, A.; El-Sayed, M. A. *J. Chem. Phys.* **1965**, *42*, 3335.
(7) Dunion, P.; Trumbore, C. N. *J. Am. Chem. Soc.* **1965**, *87*, 4211.
(8) Lee, E. K. C. *J. Phys. Chem.* **1967**, *71*, 2804.
(9) Shortridge, R. G., Jr.; Rusbult, C. F.; Lee, E. K. C. *J. Am. Chem. Soc.* **1971**, *93*, 1863.
(10) Blades, A. T. *Can. J. Chem.* **1970**, *48*, 2269.
(11) Whitlock, R. F.; Duncan, A. B. F. *J. Chem. Phys.* **1971**, *55*, 218.
(12) Svendsen, E. N.; Vala, M. T. *Acta Chem. Scand.* **1972**, *26*, 3475.
(13) Mirbach, M. F.; Mirbach, M. J.; Kon-Chang Liu; Turro, N. J. *J. Photochem.* **1978**, *8*, 299.
(14) Cansley, G. C.; Russel, B. R. *J. Chem. Phys.* **1980**, *72*, 2623.
(15) Lee, E. K. C.; Lewis, R. S. *Adv. Photochem.* **1980**, *12*, 72.
(16) Michl, J. *Mol. Photochem.* **1972**, *4*, 243, 257, 287.
(17) Turro, N. J. "Modern Molecular Photochemistry"; Benjamin-Cummings: Menlo Park, CA, 1978.
(18) Nanda, D. N.; Jug, K. *Theor. Chim. Acta* **1980**, *57*, 95, 107, 131.
(19) Himmelblau, D. N. "Applied Nonlinear Programming"; McGraw Hill: New York, 1972.
(20) Jug, K.; Hahn, G. *J. Comput. Chem.* **1983**, *4*, 410.

0002-7863/84/1506-2538$01.50/0

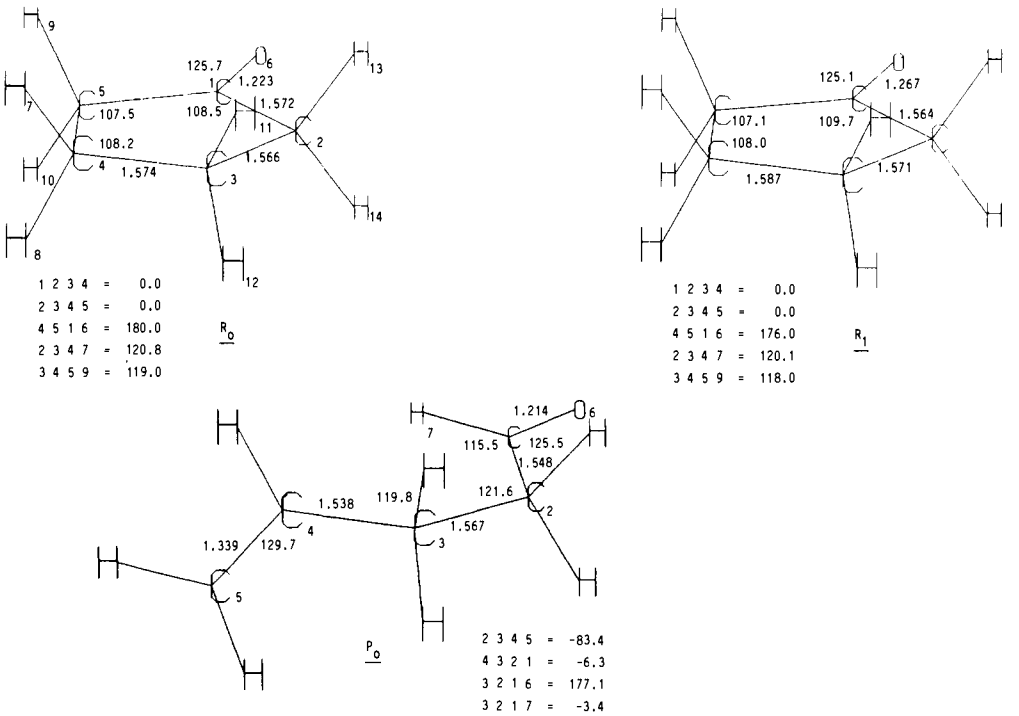

Figure 1. Geometries (Å, deg) for ground and excited singlet states R_0, R_1 of cyclopentanone and P_0 of 4-pentenal.

it may be classified as one of n type. In the Koopmans' approximation, the calculated ionization potential of CP is 9.45 eV which compares closely with the experimental value 9.34 eV.[14]

The lowest unoccupied MO (LUMO) of CP is also localized on the CO group in the equilibrium geometries of R_0 and R_1; the extent of this localization is more on C than on O. Further, the LUMO of CP is purely of σ^* type in R_0; this character is maintained in R_1.

The orbital next to LUMO is of π^* type in the equilibrium geometries of both states R_0 and R_1, and this orbital is also localized on the CO group. In its equilibrium geometry, the state R_1 is mainly composed of the excitation from the HOMO to the orbital next to LUMO; therefore, this state of CP must be assigned as n–π^*. It is in agreement with experiment.[6] The calculated singlet excitation energy of the molecule is about 1 eV higher than the experimental value, which can be estimated to be larger than 350 nm.[4] However, for adiabatic excitation energies, disagreements of this order of magnitude between theory and experiment are not uncommon.[21,22]

The small difference between the vertical singlet and triplet energies indicates a consistent shift for both states compared with experiment. The calculated first triplet and singlet excitation energies of 4P, corresponding to those where there are no experimental results available, are appreciably larger than the excitation energies of CP.

3.2. Geometries of All Relevant Equilibria. The equilibrium geometries of ground states R_0 and P_0 and excited state R_1 of CP and 4P are presented in Figure 1. In R_0 the oxygen atom is coplanar with the carbon ring. The point group is C_{2v}. All CC bond lengths are nearly equal, in agreement with experiment.[14] Compared to the ground state the CC bond lengths are only slightly changed in R_1, but the CO bond length is increased and the CO group is bent out of the ring plane due to a n–π^* excitation. R_1 belongs to point group C_s. In 4P the group state P_0 is devoid of any symmetry with the "ene" group perpendicular to the plane of the other atoms.

Figure 2 shows the fully optimized geometries of three different triplet and one singlet intermediates. The three triplet intermediates belong to the lowest triplet surface at their optimum geometry. These states will be denoted in the following as $^3I_1$, $^3I_1'$, $^3I_1''$, and I_1. All three triplet geometries are significantly different from those of R_0 and R_1. $^3I_1''$ with nonplanar C_s symmetry has the closest similarity of the three to R_0 and R_1. The CC bonds in α,α' position to the carbonyl group have bond lengths of 1.704 Å and consequently a bond order[23] of 0.8, less than a single bond. The CC bonds in β,β' position are substantially shorter with 1.543 Å. Because of the expanded CC bonds lengths in α,α' position this minimum is not in the Franck–Condon zone. There is no other triplet minimum which we could label $^3R_1$. $^3I_1'$ has a planar C_1 geometry with an expanded C_α–CO bond of 2.554 Å and a very small bond order of 0.15. It is remarkable that the remaining CCO group is bent. The lowest intermediate, $^3I_1$, has, in addition, the methylene group rotated by 87° out of the original ring plane. As a consequence, hydrogen atom H_7 is almost in the plane $C_1C_2C_3C_4$ with a distance H_7C_1 of 2.69 Å. The bond order of C_1C_5 is now zero. There is a transition state for the rotation of the methylene group about the C_3C_4 bond corresponding to $^3I_1$ on the ground state surface. In the singlet intermediate I_1 there is degeneracy of the n–σ^* and n–π^* excitations. The significant difference from the triplet states is that the C_5C_1O group is nearly linear. The bond order is 0.86 for C_5C_1 and 0.66 for C_2C_1, so these bonds are still substantial.

Figure 3 shows two diradical situations $^{1,3}D$ and $^{1,3}D'$, where the CO group is practically dissociated. It should be noticed that the geometries of the carbon fragments are identical with those for the planar first transition state and the twisted first intermediate of the cyclobutane pyrolysis.[24] Finally, Figure 3 shows the geometry of transition state TS_0 for hydrogen migration of $^3I_1$ to P_0. Here we find a planar, almost symmetric, five-membered ring. The hydrogen atom H_7 has bond orders of 0.64 for H_7C_1 and 0.60 for H_7C_4; hence it is almost equally shared between C_1 and C_4.

Figure 4 contains MO diagrams relevant to the following discussion.

3.3. Potential Surfaces and Reaction Mechanisms. Figure 5 serves as the starting point for a discussion of the reaction mechanisms. It presents the relevant energy surfaces for S_0, S_1, T_1, and T_2 when a photochemical reaction is initiated from CP. One recognizes the minimum of R_1 above R_0, a conical intersection

(21) Mishra, P. C.; Jug, K. *Theor. Chim. Acta* **1982**, *61*, 559.
(22) Schweig, A.; Thiel, W. *J. Am. Chem. Soc.* **1981**, *103*, 1425.
(23) Jug, K. *J. Am. Chem. Soc.* **1977**, *99*, 7800; Theor. *Chim. Acta* **1979**, *51*, 331.
(24) Jug, K.; Müller, P. L. *Theor. Chim. Acta* **1981**, *59*, 365.

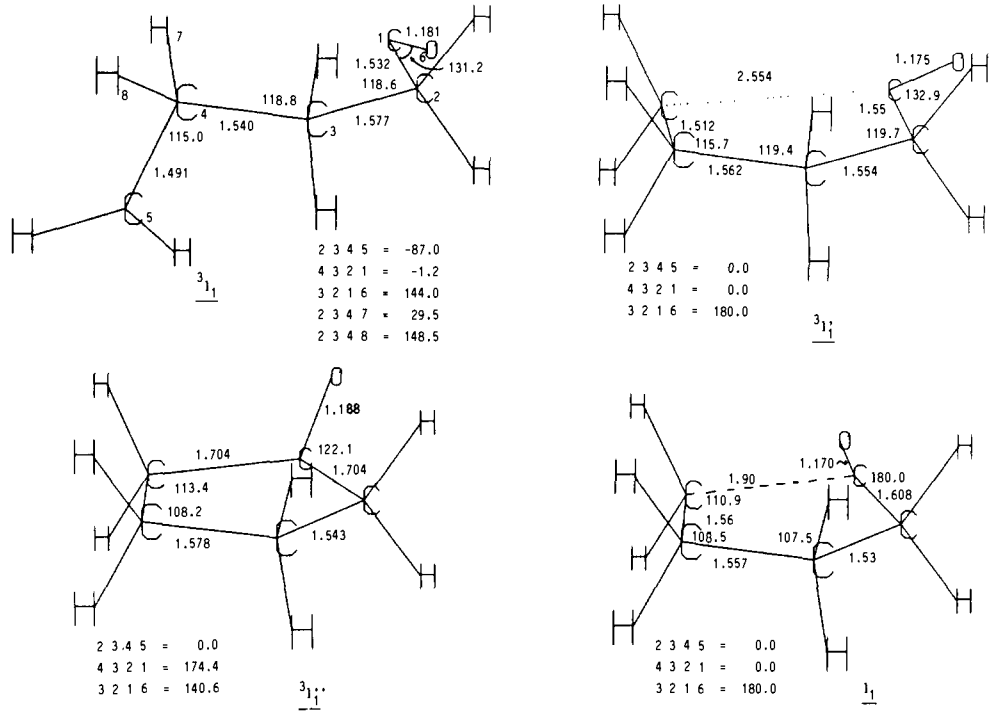

Figure 2. Geometries (Å, deg) of three triplet intermediates $^3I_1$ and one singlet intermediate I_1 on the lowest excited state surfaces.

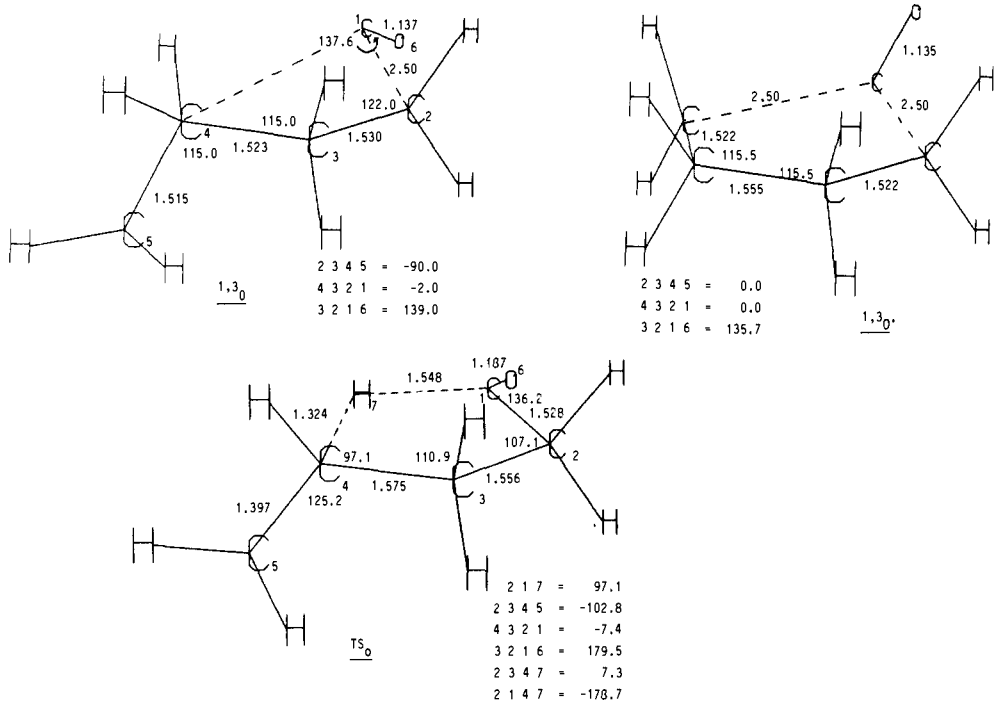

Figure 3. Geometries (Å, deg) of diradical situations D near photofragmentation and transition state TS_0 for hydrogen migration.

of T_1 and T_2 surfaces, and low-lying triplet intermediate $^3I_1$, almost degenerate with the S_0 surface. From this figure it is apparent that a molecule excited to the S_1 surface has the following possibilities to leave this surface: (1) fluorescence to the ground state, (2) intersystem crossing (ISC) to T_1, (3) ISC to T_2. These mechanisms are discussed in the following by two-dimensional cuts through the potential hypersurfaces along a coordinate relevant for the reaction pathway.

Figure 6 aids us in understanding the molecular motion on the singlet surfaces. We concentrated the energy optimization on the repulsive $R_2(n-\sigma^*)$ state, which crosses the $R_1(n-\pi^*)$ state during the α-cleavage process under conservation of C_s symmetry. This crossing generates the lowest lying transition state on the first excited singlet surface. The barrier of over 2 eV is too high to be overcome by vibrational motion. This is in agreement with the experimental finding that the fluorescence quantum yield is independent of temperature. We therefore have to identify this barrier with that one theoretically postulated.[17] Pathways along avoided crossings lead to symmetry reduction to C_1 and higher order transition states. They are not shown in the figure. If one considers the triplet states vertically below the first excited singlet curve, one notices another interesting aspect. Starting with the assumption that the molecule is in a high-lying vibrational state of S_1 and that it has a lifetime of more than 10^{-11} s, we cannot exclude ISC processes to hot triplet states with planar expanded geometry. The calculations show that the processes, including subsequent internal conversion (IC), lead to planar triplet intermediates (dashed curve) and have predissociative character.

We now turn again to Figure 5. We see that there are two principally different possibilities for intersystem crossing in the

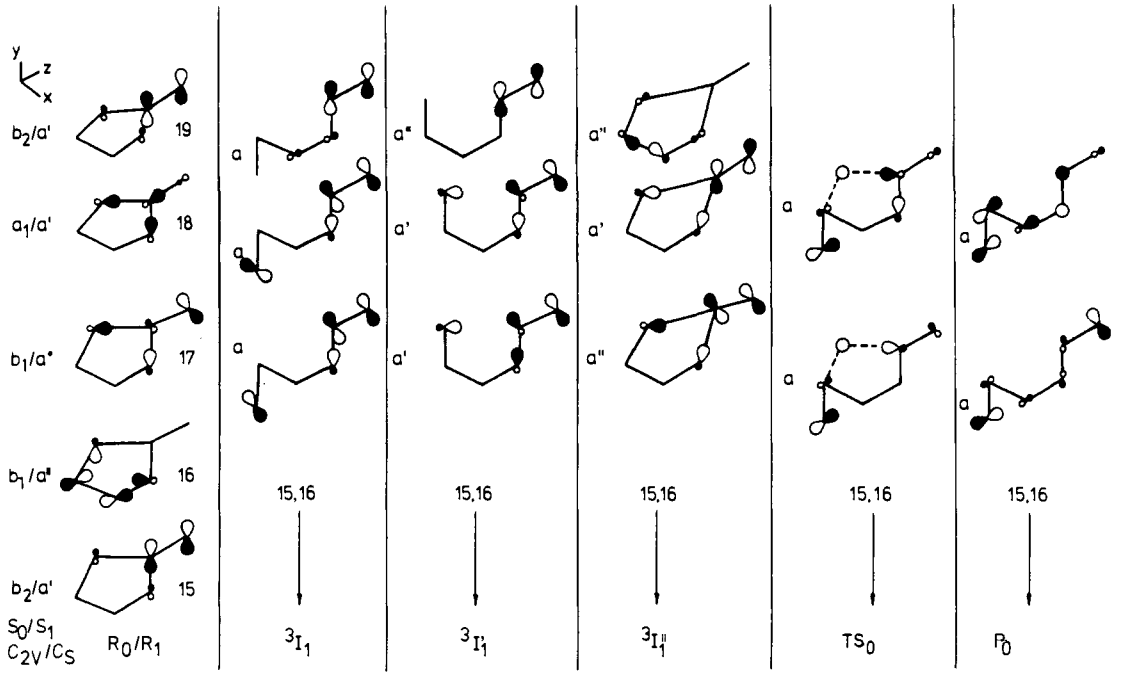

Figure 4. Relevant MOs of reactant and intermediates.

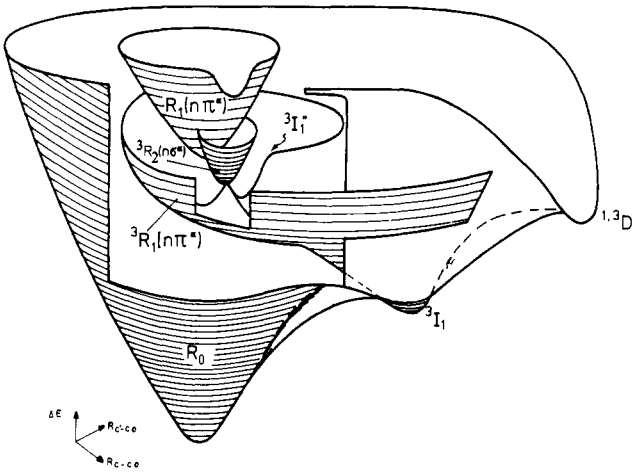

Figure 5. Potential surfaces for initial photoreaction of cyclopentanone along CC bond lengths with energy optimized extrema.

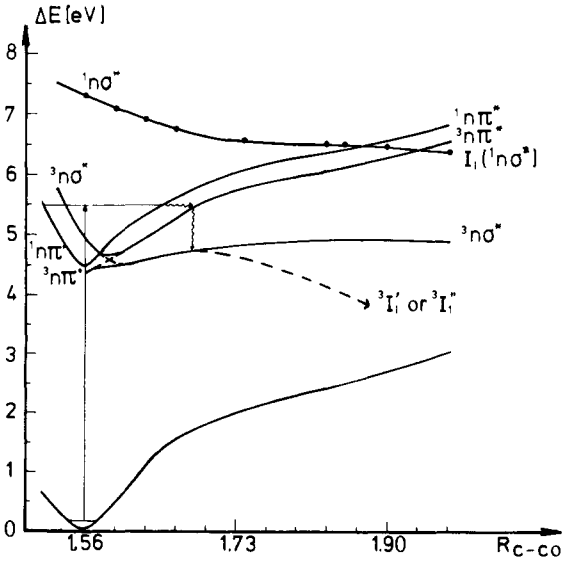

Figure 6. Potential curves interpolated between vertical $R_0 \rightarrow R_1$ excitation and I_1 equilibrium: ●, points of optimized geometry.

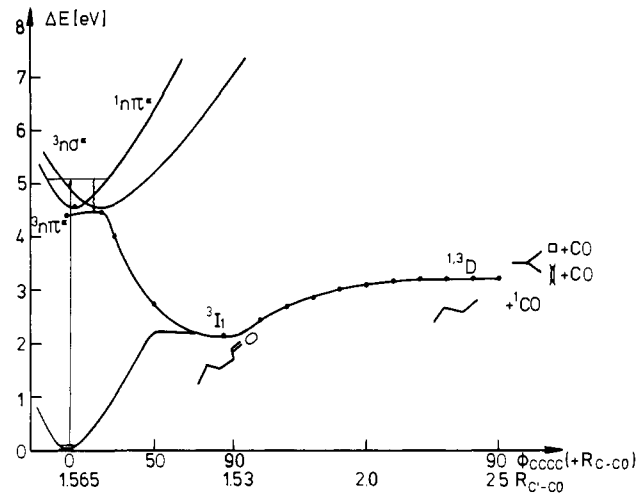

Figure 7. Potential curves for double α-cleavage of cyclopentanone to a twisted diradical $^{1,3}D$: ●, points of optimized geometry.

neighborhood of the R_1 equilibrium. A transition can lead to either $^3R_2(n-\sigma^*)$ or $^3R_1(n-\pi^*)$. We discuss first the motion to the predissociative surface $^3R_2(n-\sigma^*)$ and the resulting mechanistic consequences. This transition can take place from almost any S_1 vibrational mode. A small deformation of the molecule under conservation of C_s symmetry suffices to invoke a crossing of $^3R_2$ and $^3R_1$ which is represented as a conical intersection (CIS) in the figure. Reduction to C_1 symmetry, i.e., no symmetry at all, leads to an avoided crossing. The IC processes implied here lead to the three intermediates $^3I_1$, $^3I_1'$, and $^3I_1''$ depending on which normal mode dominates at the triplet–triplet transition. Since the manifold of subsequent IC processes cannot be completely represented in one three-dimensional figure, we use again two-dimensional plots to analyze the mechanism.

Figure 7 shows the potential curves for a pathway which leads to the completely dissociated diradical products $^{1,3}D$. This mechanism passes through the diradical intermediate $^3I_1$ with a relative energy of 2.2 eV. Diradicals are defined in the sense of Salem and Rowland.[25] To understand the origin of the $^3I_1$ minimum, we refer to the MO diagram of Figure 4. $^3I_1$ results

(25) Salem, L.; Rowland, C. *Angew. Chem.* **1972**, *84*, 86.

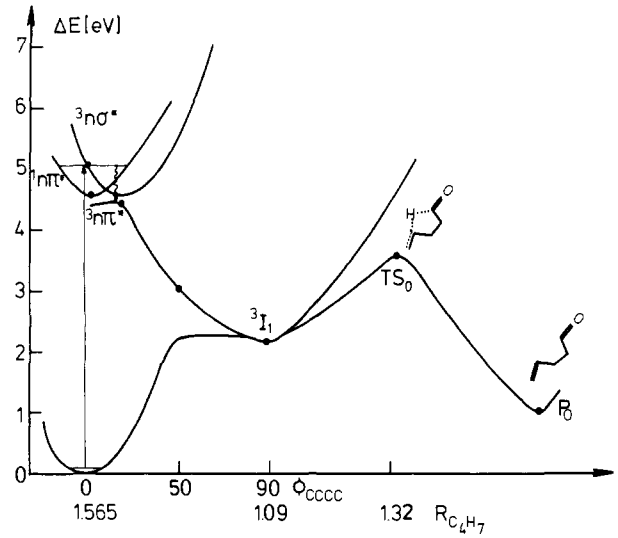

Figure 8. Potential curves for hydrogen migration of cyclopentanone to 4-pentenal: ●, points of optimized geometry.

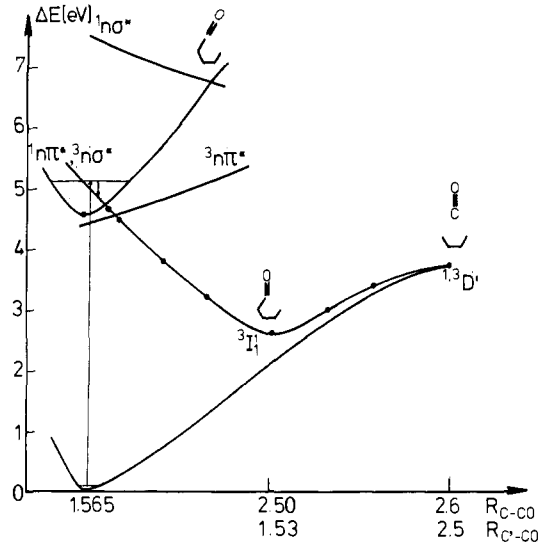

Figure 9. Potential curves for double α-cleavage of cyclopentanone to a triplet intermediate $^3I_1'$: ●, points of optimized geometry.

from a HOMO–LUMO excitation. Both orbitals are strong mixtures of σ and π parts and belong to irreducible representation a. It can be concluded that $^3I_1$ is the result of an avoided crossing of the originally pure $^3R_2(n-\sigma^*)$ and $^3R_1(n-\pi^*)$ triplet surfaces. ISC from $^1R_1(n-\pi^*)$ to $^3R_2(n-\sigma^*)$ with subsequent IC to $^3R_1(n-\pi^*)$ through an avoided crossing yields the diradical intermediate $^3I_1$. One can further conclude from Figure 7 that an additional energy of 1 eV is necessary to obtain the completely dissociated products $^{1,3}D$.

From the geometry of $^3I_1$ it can be seen that it offers a possibility to reach 4P. This mechanism is represented in Figure 8. A removal of the degeneracy after ISC leads over a barrier of 1.3 eV to P_0 of 4P in a twisted conformation. We find that this is the energetically most favorable pathway to 4P.

It should be stated, however, that a molecule in state $^3I_1$ will most likely return to the ground state R_0 of CP. This is in agreement with experimental facts according to which CP is the main product of its photolysis.[5]

There are two reasons why the subsequent reactions are still involved in the process. Firstly, the CIS point is energetically higher than the transition state TS_0 and the diradicals $^{1,3}D$ and $^{1,3}D'$ so that these can be overcome before relaxation to the $^3I_1$ state takes place. Secondly, the triplet surface crosses the S_0 potential surface above $^3I_1$ for vibrational modes of S_0 above the barrier. From the energy barriers of this calculation there is no obvious preference for isomerization to 4-pentenal as compared

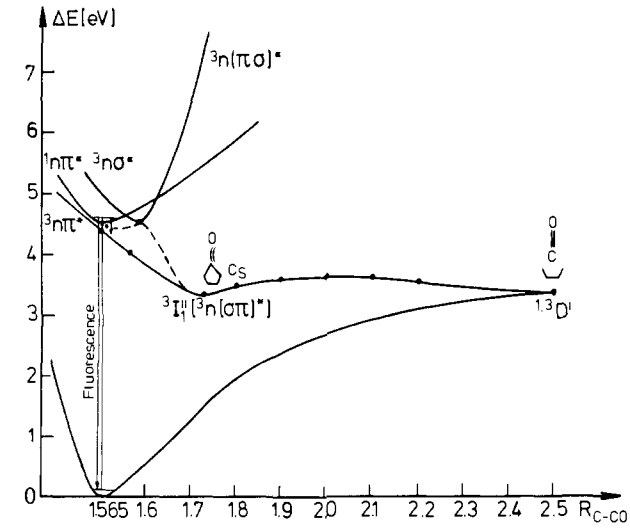

Figure 10. Potential curves for double α-cleavage of cyclopentanone to a planar diradical $^{1,3}D'$: ●, points of optimized geometry.

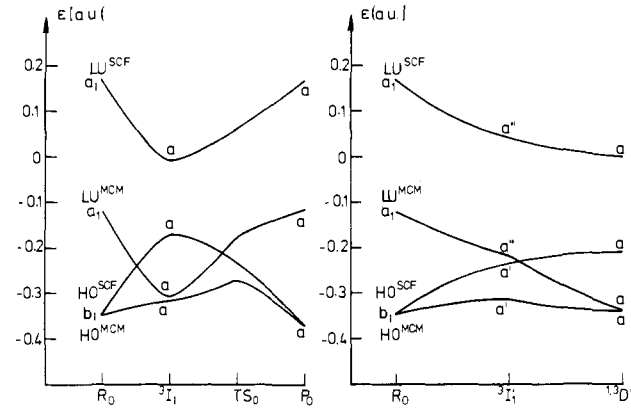

Figure 11. Correlation diagram of (a) photoisomerization of cyclopentanone to 4-pentenal and (b) photofragmentation to two ethylene and CO based on MCM molecular orbitals.

to fragmentation in CO and cyclobutane or two ethylene with decreasing excitation energy. However, from $^3I_1$ the tunnel effect can enhance the rate of hydrogen migration to 4-pentenal.

We now discuss the mechanisms which can result from the remaining ISC processes. Figure 9 shows potential curves focusing on the minimum $^3I_1'$ with an energy of 2.62 eV. This state is due to an $n-\sigma^*$ excitation as can be seen from Figure 4. The potential curve shows that it correlates directly with $R_2(n-\sigma^*)$ vertical above R_0. We conclude that the minimum $^3I_1'$ can be reached under conservation of C_s symmetry via the conical intersection. This minimum, which is not degenerate with the ground state, opens a channel to the planar diradical $^{1,3}D'$ with a barrier of 1.5 eV. Because of steric effects, there is no pathway from $^{1,3}D'$ to isomerization.

The final set of potential curves is in Figure 10. The lowest triplet has a very flat minimum $^3I_1''$ of C_s symmetry at 3.35 eV. From this state, the completely dissociated products $^{1,3}D'$ can be reached with a very low barrier of less than 0.2 eV. This process can be concerted or nonconcerted via $^3I_1''$. The MOs in Figure 4 show that $^3I_1''$ is the result of a mixed $n-\sigma^*$ and $n-\pi^*$ excitation. This observation and the fact that this state has C_s symmetry lead us to conclude that the intermediate $^3I_1''$ can be reached by ISC from $^1R_1(n-\pi^*)$ to $^3R_2(n-\pi^*)$. Since this process is in competition with fluorescence, the mechanism seems to be the least likely.

All discussed reactions are thermally forbidden since they lead, with the exception of the second isomerization step, to states which would be involved in the nonconcerted symmetry-forbidden cyclobutane pyrolysis. We have investigated all possible thermally induced reaction pathways and find that they lead, with no exception, to diradicals. These states have symmetry-dependent

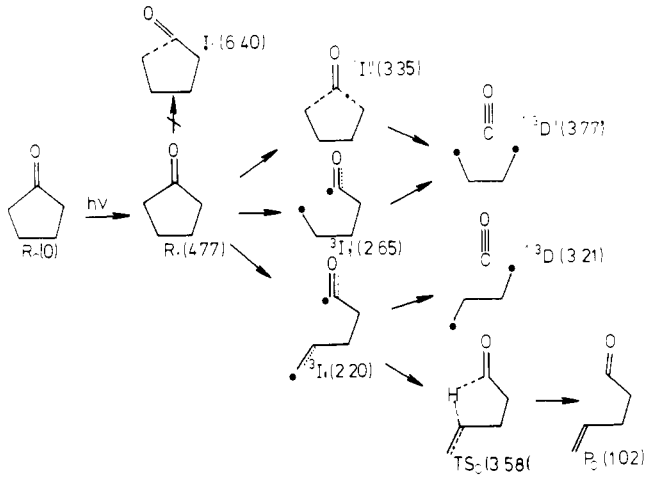

Figure 12. Schematic representation of cyclopentanone photoreaction mechanism.

quasi-degeneracy of HOMO and LUMO as can be seen from Figure 11. We have taken here two representative reactions and calculated their MO correlation diagrams with a multiconfigurational variation of moments (MCM) method.[26] These correlation diagrams show that thermal isomerization and fragmentation are Woodward–Hoffmann forbidden.[27]

A schematic survey of our results is presented in Figure 12. The figure shows the sequence of steps from reactant to products. The two diradicals ^{1,3}D and ^{1,3}D′ finish with formation of cyclobutane or two ethylene and CO.

4. Conclusion

In this investigation we have clarified the mechanism of photochemical reaction of cyclopentanone to three different products. We have presented the various pathways for photoisomerization to 4-pentenal and for photofragmentation to cyclobutane or two ethylene and CO. In all reactions excitation is followed by intersystem crossing and internal conversion. Cyclopentanone is usually the main product due to fluorescence and relaxation to the lowest triplet intermediate $^3I_1$. The products P_0, ^{1,3}D, and ^{1,3}D′ are obtained if reaction can take place before relaxation to $^3I_1$. At high excitation energies the main products are cyclobutane or two ethylene and CO in the ground state. With decreasing excitation energies, 4-pentenal is also formed.

Acknowledgment. This work was partly supported by Deutsche Forschungsgemeinschaft. One of us (P.C.M.) thanks Alexander von Humboldt-Stiftung for a fellowship. The calculations were performed with a CYBER 76 at Universität Hannover.

Registry No. Cyclopentanone, 120-92-3.

(26) Müller-Remmers, P. L.; Jug, K. *J. Am. Chem. Soc.*, submitted for publication.

(27) Woodward, R. B.; Hoffmann, R. "The Conservation of Orbital Symmetry", Verlag Chemie: Weinheim, 1971.

Properties and Reactions of Organometallic Fragments in the Gas Phase. Ion Beam Studies of FeH^+

L. F. Halle, F. S. Klein,[1] and J. L. Beauchamp*

Contribution No. 6813 from the Arthur Amos Noyes Laboratory of Chemical Physics, California Institute of Technology, Pasadena, California 91125. *Received July 28, 1983*

Abstract: Analysis of the thresholds for the reactions of Fe^+ with H_2 and D_2 studied with an ion beam apparatus yield the bond dissociation energy $D°(Fe^+–H)$ = 59 ± 5 kcal/mol. From this bond strength the proton affinity of an iron atom, PA(Fe) = 190 ± 5 kcal/mol, is calculated. Ion beam studies of the deprotonation of FeH^+ by bases of various proton affinities are consistent with this value. Hydride transfer reactions of these bases with FeH^+ yield a lower limit for the hydride affinity of FeH^+, $D°(HFe^+–H^-)$ > 232 kcal/mol. These energetics indicate that oxidative addition of H_2 to an iron atom is exothermic by at least 22 kcal/mol. The nearly thermoneutral formation of FeD^+ in the reaction of FeH^+ with D_2 occurs only with a small cross section at higher energies and exhibits a threshold of 20 ± 7 kcal/mol. If oxidative addition of D_2 to iron precedes reductive elimination of HD, then this activation energy implies a significant barrier for formation of an Fe(IV) intermediate. Alternatively, if the exchange process involves a four-center transition state, the observation of a significant activation energy is consistent with recent theoretical predictions that such processes are unfavorable if the metal–hydrogen bond has predominantly metal s or p character. Correlations of experimental bond energies with promotion energies provide evidence that the $Fe^+–H$ bond is primarily metal s in character. Formation of FeD^+ is observed with a moderate cross section at low energies in the reaction of FeH^+ with ethene-d_4. This results from reversible olefin insertion into the metal hydrogen bond, a process which does not involve higher oxidation states of iron. Reactions of FeH^+ with several alcohols, aldehydes, ethers, and alkanes are also presented. Facile oxidative addition reactions to C–C and C–H bonds of alkanes do not occur at low energies, presumably owing to the requisite formation of an Fe(IV) intermediate. The reactions of FeH^+ with the oxygenated compounds are generally of the type expected for strong Lewis acids.

Introduction

Activation of molecular hydrogen by a metal center is an important step in catalytic processes both in solution and on surfaces.[2] Because of this, the properties and reactivity of the intermediate metal hydrides are of great interest. Additional interest stems from the observation of diatomic metal hydrides, such as FeH, in spectra of stellar atmospheres.[3,4] These species have been

(1) On leave from the Weizmann Institute, Rehovot, Israel.
(2) Vaska, L.; Werneke, M. F. *Trans. N. Y. Acad. Sci., Ser. 2* **1971**, *33*, 70, and references therein.
(3) Smith, R. E. *Proc. R. Soc. London, Ser. A* **1973**, *332*, 113.
(4) Wing, R. F.; Ford, W. K. *Publ. Astron. Soc. Pac.* **1969**, *81*, 527.

0002-7863/84/1506-2543$01.50/0